


Article

A Virtual Test Bench of a Parallel Hybrid Propulsion System for UAVs

Luca Boggero [†], Sabrina Corpino [†], Andrea De Martin ^{*,†}, Giuseppe Evangelista [†], Marco Fioriti [†] and Massimo Sorli [†]

Department of Mechanical and Aerospace Engineering, Politecnico di Torino, 10129 Torino, Italy

* Correspondence: andrea.demartin@polito.it

† These authors contributed equally to this work.

Received: 4 June 2019; Accepted: 27 June 2019; Published: 2 July 2019



Abstract: The article proposes the design of a test bench simulator to test a parallel hybrid propulsion architecture for aeronautical applications. The virtual test bench simulates, in a scaled version, the real test bench, designed for a power of about 0.4 MW. After presenting the architecture of the real propulsion system, the virtual test bench is described. The real system is basically composed by a paralleled electric motor and thermal engine which provide mechanical power to the propeller. Saving cost and volume the test bench is composed by electric motors simulates the behaviors of the real propulsion system despite their differences. The dynamic relationships expressing the transmission of torque between the components, and the method of down-sizing the power delivered are highlighted. Particular attention is given to the real inertia actions that must be simulated on the virtual test bench. An application of the proposed methodology is then presented through the simulation of the take-off phase, and the torque time histories, angular velocities and powers generated on the virtual test bench are used to verify the corresponding time histories expected in the real system.

Keywords: virtual test bench; hybrid propulsion; UAV

1. Introduction

The hybrid-electric propulsion is rather innovative technology used to combine the mechanical power generated by one (or more) electric drives with a thermal engine. It can be safely considered a mature and widely used solution in the automotive field, where it is emerging due to environmental concerns and he associated with the reduction of the operating costs due to the lower fuel consumption [1]. Similar advantages are expected in the aeronautics field, where the application are still few and mostly limited to UAVs. In recent years a number of studies on the subject have been published, including several theoretical studies [2–7], definition of test benches [8–10] and aircraft prototypes [11,12]. So far, the majority of the available literature is focused on the design and the performance analysis of one of two alternative architectures: the serial hybrid configuration and the parallel one. The serial hybrid solution is peculiar of the Diamond DA36 E-Star, the first aircraft equipped with a hybrid-electric propulsion system. In this solution, the thermal engine provides the mechanical power to an electrical generator, which hence supplies the electrical drive and its batteries [11]. This architecture might be however not suitable for short haul airplanes, since it can excessively increase the mass of the propulsion system due to the several power conversion steps [5]. The use of a parallel architecture, in which the two power sources are independently generated and combined through a gearbox, is then particularly attractive as it might entail a lighter propulsion system. Moreover it would allow to exploit different combinations of the two power sources to achieve the most efficient solution as a function of the operating conditions. In example, it could be possible to add the contribution of both the electric motor and the thermal engine during the maximum power

demand, allowing a procedure known as powerboost, or using only the electric motor during less demanding mission segments, like the taxi mode.

The development of a hybrid propulsion system usually starts from a conceptual design of a hybrid aircraft given a set of high-level requirements. A rigorous methodology aimed at this conceptual design, starting from trade-off studies [6], is provided in [7]. The preliminary results of these analyses are then employed for the initial assessment of the components installed within the hybrid propulsion system, namely the propeller, the mechanical transmission, the internal combustion engine (ICE), the electrical machine, the batteries and the system controller. This assessment is preliminarily done through virtual models of the real components, which are aimed at investigating the transient and steady states. Furthermore, the integration of the components is evaluated through these virtual models, determining the connection and the exchange of parameters—e.g., torques, electric currents and gear ratios—and simulating the entire system. The development process can then proceed with the manufacture of a first system prototype or test bench, which is required for the performance assessment and then the certification of the new product.

Although a significant number of test bench architectures have been presented in the automotive field [13,14], only a handful of prototypes of aeronautical hybrid propulsion systems have been proposed. Flight Design's test prototype presented in [10] is a 1:1 mock-up version of a real hybrid parallel system. In this test bench, a 4-cylinder 1200 cm³ Rotax 914 thermal engine is connected through a Poly-V belt with a synchronous permanent magnet electric motor. As the ICE reaches 85.8 kW and the peak power of the electrical machine (EM) amounts to 30 kW, the system is designed to generate a surplus of propulsive power during the simulation of certain phases of the mission profile, as the take-off (powerboost functionality). In this condition, the EM is supplied by a 21 Ah lithium-iron-phosphate (LiFePO₄) battery pack characterized by an electric voltage of 130 V. The hybrid system test bench is eventually completed by an electronic controller, aimed at monitoring and managing the power demand of each component. Although extremely useful as technological demonstrators, 1:1 prototypes are usually too expensive and too complex to manage during the early phase of the development activities. As such, scale-down benches have also been proposed. In [8], for instance, the hybrid drive is obtained connecting a 1.18 kW gasoline engine with a nearly 0.7 kW DC brushless EM. The ICE and the EM both move a variable speed propeller through a fixed 1:1 gear ratio. This test bench allows the simulation of the powerboost and the traditional flight—i.e., the EM operating as generator—functionalities. Furthermore, for safety and economic reasons, the behavior of certain components might be simulated installing other kinds of equipment, for instance replacing the thermal engine with an EM, or simulating the behavior of a component by means of a virtual model. A similar approach is presented also in [9] for a UAV application.

The virtualization of part of the test bench is pretty common in the automotive field, as reported in [14], where the electric energy storage has been replaced with a software-in-the-loop. The same procedure is usually applied in complex aeronautic test benches and Iron Birds, where aerodynamic forces acting on flight control surfaces are often reproduced by an hydraulic servo-actuator suitably controlled by a dedicated software [15,16], while it is still rather uncommon for propulsion systems.

Aim of the presented study is the definition of an original methodology for the development of a virtual test bench for a hybrid propulsion system working close to 0.4 MW to be applied to a new UAV under development. After presenting the architecture of the real propulsion system, consisting essentially of an ICE, an EM, a gearbox (G), a propeller (P), a battery (B), the virtual test bench composed by three electric servomotors (EM1, EM2 and EM3) and by the battery simulator is described. The dynamic relationships expressing the transmission of torque between the components, and the method of down-sizing the power delivered are highlighted. Particular attention is given to the real inertia actions that must be simulated on the virtual test bench. The simulation of the take-off flight phase is then proposed, and the obtained results are used to verify the corresponding time histories expected in the real architecture. In the conclusive section, limitations and possible future developments of the proposed work are presented.

2. General Overview of the Virtual Test Bench

A virtual test bench is a simulation environment developed before the real test bench to support its design according to a model-based philosophy and to verify its results once it is made available.

Like real test benches, virtual test benches might be scaled down for different reasons such as space management and cost. An important parameter is the scale factor, which is the ratio between the power installed on the test bench—virtual or physical—and the power installed on the real propulsion system. Being defined and supported by analytical relationship, it allows one to emulate the real system behavior under both static and dynamic conditions. To this end, not only the installed power shall be scaled, but also the physical inertia of each component. This last aspect is particularly important during the study of transitory behaviors such as the startup of the thermal engine, sometime performed by exploiting the inertia of the propeller without adopting a dedicated starter equipment.

Moreover, according to the specifications of the aircraft, a virtual bench may be used for the verification of the degree of hybridization, which is meant as the ratio among the propulsive power generated by the electric drive over the total propulsive power. Therefore, the best solution in terms of fuel consumption, weight and energy management might be defined. More generically, the architecture of the test bench meant as the integration and the interconnection of all the system components might be more appropriately assessed through a virtual model.

Starting from a set of initial specifications of the aircraft, a virtual test bench provides a reliable environment for predicting the impact of changes and perform upgrades. It can represent a useful and cheap tool not only for preliminary design of a physical test bench but also for the definition of the validation tests plans by simulating several test scenarios in advance. In example, the virtual test bench can be exploited to easily simulate different operative modes reported in Table 1.

Table 1. Parallel hybrid propulsion system operative mode.

Flight Phase	ICE	Electric Motor
Green Taxi	Off	Motor
Take-off (powerboost)	On	Motor
Climb	On	Motor
Cruise	On	Generator
Descent	Off	Generator
ICE heating	On	Generator

It is also true that the virtual test bench cannot replace the physical test bench in terms of certification of the test bench itself or of the results obtained, so the virtual test bench can represent only a preliminary step of the development process. In this preliminary phase, the results obtained can be considered acceptable when the behavior of the quantities derived from the simulation, is compatible with those expected in the associated flight phase.

3. Reference Architecture and Scaling Methodology

The test bench is designed to mirror the architecture of the real parallel hybrid propulsion system, which functional scheme is shown in Figure 1. The electric drive is up made of a battery, the electronic power unit (EPU) controlling the EM and a clutch used to disconnect the drive from the rest of the system if needed. The ICE is instead supplied from a fuel tank and provides power to the gearbox through another electro-mechanical clutch which can be disengaged during the green taxi operations. In the test bench, the installed power of approximately 400 kW is appropriately scaled to allow for a realistic representation of the flight conditions for different operative modes both for static and dynamic cases.

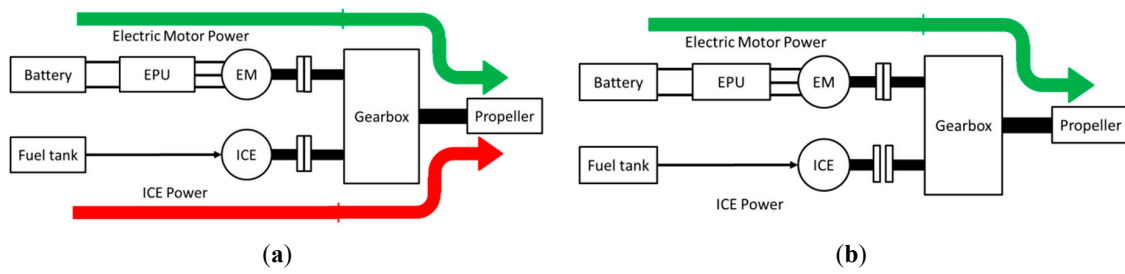


Figure 1. Functional scheme of the parallel hybrid propulsion architecture under analysis: (a) power boost conditions; (b) green taxi operations.

All the power sources acting on the system are replaced by electric motors, as shown in Figure 2, the torques provided by the ICE and by the aerodynamic load acting on the propeller are simulated by brushless motors. The use of an electric motor for the ICE simulation allows to significantly simplify the test bench installation and avoid pollution management during the tests. Although the behavior of an EM is significantly different from that of an ICE, some features such as the inertia, the typical torque ripple of the ICE and its mechanical characteristic can be effectively taken in to account via software and acting on the electric motor control.

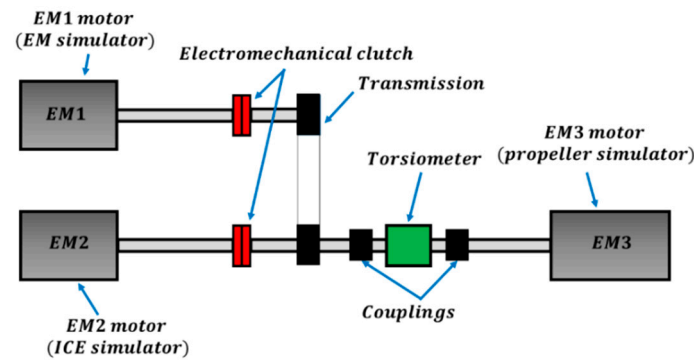


Figure 2. Functional scheme of the real test bench for the parallel hybrid propulsion architecture under analysis.

A synchronous belt transmission for the mechanical connection of the output shafts EM1 and EM2 completes the proposed architecture. Two electromechanical clutches are installed on the EM1 and EM2 output shafts. The placement of the clutch on EM1 motor shaft is justified by an easier installation, the need to measure the torque on each axis separately and to interrupt the power transmission in case of an emergency.

The clutch on the EM2 shaft allows to simulate missions when the ICE is not in operation (e.g., during taxi mode), or during simulations of the ICE startup. Defined the test bench architecture, it is possible to determine a scale factor for its components starting from the real system dimensions. For this purpose, the dynamic behavior of the real propulsion system is mathematically described for the different operating conditions. Making reference to the diagram reported in Figure 3 for power boost conditions and translating the torque contributions to the ICE axis, the dynamic equilibrium of the system can be described as:

$$T_{ICE} + T_{EM}\tau_2'\eta_2 - \left(I_{ICE} + I_P\frac{\tau_1^2}{\eta_1} + I_{EM}\tau_2'^2\eta_2 \right) \dot{\omega}_{ICE} - \left(\gamma_{ICE} + \gamma_P\frac{\tau_1^2}{\eta_1} + \gamma_{EM}\tau_2'^2\eta_2 \right) \omega_{ICE} = T_P\frac{\tau_1}{\eta_1} \quad (1)$$

where T_{ICE} is the ICE torque, T_{EM} is the EM torque and T_P is the propeller torque. I_{EM} , I_{ICE} and I_P are the inertias of the electric motor, ICE and propeller respectively, while γ_{EM} , γ_{ICE} and γ_P are the viscous damping coefficients. ω_{EM} , ω_{ICE} and ω_P are the angular speeds; τ_1 is the transmission ratio

of the mechanical transmission between propeller and ICE, defined in Equation (2), while τ'_2 is the transmission ratio between EM and ICE defined in Equation (3). Finally, we define the transmission efficiencies η_1 and η_2 (from the electric motor to the propeller):

$$\tau_1 = \frac{\omega_P}{\omega_{ICE}} \quad (2)$$

$$\tau'_2 = \frac{\omega_{EM}}{\omega_{ICE}} \quad (3)$$

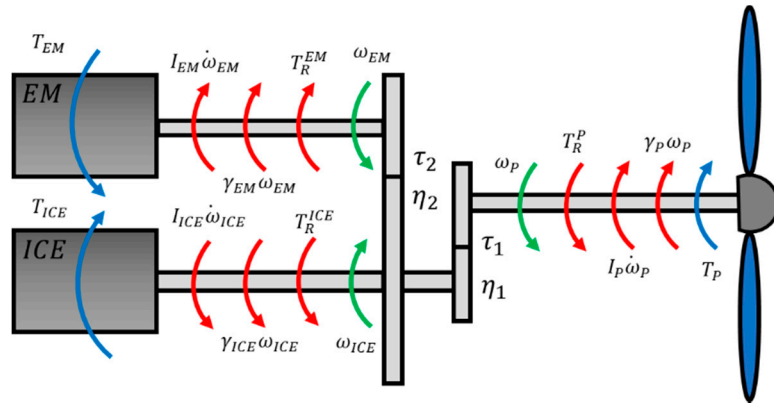


Figure 3. Torques acting on the hybrid propulsion architecture during power boost.

Similar considerations can be performed on the test bench, as depicted in Figure 4. By reporting all of the torque contributions to the EM2 axis, the equilibrium equation of the test bench can be written as:

$$T_2 + T_1\tau_{2-1}\eta_{1-2} - (I_2 + I_3 + I_1\tau_{2-1}^2\eta_{1-2})\dot{\omega}_2 - (\gamma_2 + \gamma_3 + \gamma_1\tau_{2-1}^2\eta_{1-2})\omega_2 = T_3 \quad (4)$$

where T_1 , T_2 and T_3 are the torque outputs of the three electric motors, I_1 , I_2 and I_3 are the inertias on the axis EM1, EM2 and EM3 and γ_1 , γ_2 , γ_3 are the viscous damping coefficients.

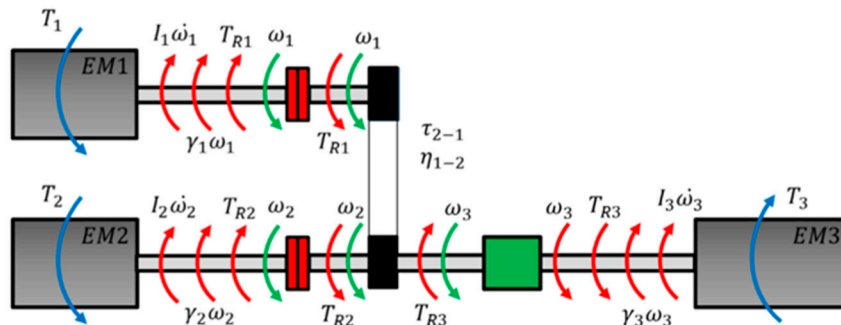


Figure 4. Torques acting on the real test bench for the hybrid propulsion architecture under analysis during power boost.

ω_1 , ω_2 and ω_3 are the angular speeds, while η_{1-2} is the belt transmission efficiency from EM1 to EM2 and τ_{2-1} is the transmission ratio between EM1 and EM2, described by Equations (5) and (6).

$$\eta_{1-2} = \frac{T_{R2}\omega_2}{T_{R1}\omega_1} \quad (5)$$

$$\tau_{2-1} = \frac{\omega_1}{\omega_2} \quad (6)$$

Defining the power scale factor k_s , the servomotors power can be written as:

$$\begin{cases} k_s = \frac{P_{EM2}}{P_{ICE}} \\ P_{EM1} = P_{EM} \cdot \frac{P_{EM2}}{P_{ICE}} \\ P_{EM3} = P_{EM2} + P_{EM1} \cdot \eta_{1-2} \end{cases} \quad (7)$$

The value of the power scale factor can be freely defined and used to down-size the real and the virtual test bench compared to real system dimensions. Since the scaling process is supported by analytical equations, it can be easily updated according to specific contextual needs.

In order to reproduce the dynamic behavior of the real propulsion system, the contribution of inertia must be scaled as well. This is done by equating the mechanical power associated with the acceleration of each movable axis on the real system with the scaled power associated with each correspondent axis on the test bench. The equivalent moments of inertia at the three axis of the real test bench, and hence the values to be used for its virtualization, can be computed as:

$$I_1 = \frac{I_{EM} \cdot \tau_2'^2 \eta_2 \cdot \dot{\omega}_{ICE} \cdot \omega_{ICE} \cdot k_s}{\dot{\omega}_2 \cdot \omega_2 \cdot \tau_{2-1}^2 \cdot \eta_{1-2}} \quad (8)$$

$$I_2 = \frac{I_{ICE} \cdot \dot{\omega}_{ICE} \cdot \omega_{ICE} \cdot k_s}{\dot{\omega}_2 \cdot \omega_2} \quad (9)$$

$$I_3 = \frac{I_P \cdot \frac{\tau_1^2}{\eta_1} \cdot \dot{\omega}_{ICE} \cdot \omega_{ICE} \cdot k_s}{\dot{\omega}_2 \cdot \omega_2} \quad (10)$$

where I_1 , I_2 and I_3 represent the moments of inertia that the virtual rig should have to ensure the dynamic equivalence. Each of these terms can be considered as the sum of the servomotors inertia I_{EM1} , I_{EM2} and I_{EM3} and of the additional inertias I_{s1} , I_{s2} and I_{s3} :

$$I_{s1} = I_1 - I_{EM1} = \frac{I_{EM} \cdot \tau_2'^2 \eta_2 \cdot \dot{\omega}_{ICE} \cdot \omega_{ICE} \cdot k_s}{\dot{\omega}_2 \cdot \omega_2 \cdot \tau_{2-1}^2 \cdot \eta_{1-2}} - I_{EM1} \quad (11)$$

$$I_{s2} = I_2 - I_{EM2} = \frac{I_{ICE} \cdot \dot{\omega}_{ICE} \cdot \omega_{ICE} \cdot k_s}{\dot{\omega}_2 \cdot \omega_2} - I_{EM2} \quad (12)$$

$$I_{s3} = I_3 - I_{EM3} = \frac{I_P \cdot \frac{\tau_1^2}{\eta_1} \cdot \dot{\omega}_{ICE} \cdot \omega_{ICE} \cdot k_s}{\dot{\omega}_2 \cdot \omega_2} - I_{EM3} \quad (13)$$

The additional inertias can be introduced in the test bench in two different ways. The first one is to mount physical inertias equal to I_{s1} , I_{s2} and I_{s3} on the motor axis EM1, EM2 and EM3. This approach is commonly used in test benches of flight servo-actuators, where the inertia of the flight control surface is simulated by an adjustable mass, but has the drawback of needing additional space on the real test bench [16].

The second solution is to embed the influence of these additional inertias within the command system by modifying the reference signals provided to the electric motors. This approach however requires high-performing torque control of the motors and increase the complexity of the test bench software and is as such discarded.

The procedure to properly scale the real test bench is then an iterative process, as shown in Figure 5; once that a certain scaling factor is selected, the bench components and their inertia must be chosen properly and their behavior compared to the expected characteristics of the real propulsion system. The iterative nature is due to the selection of commercial components, which characteristics are inevitably slightly different from the ones demanded by the scaling procedure.

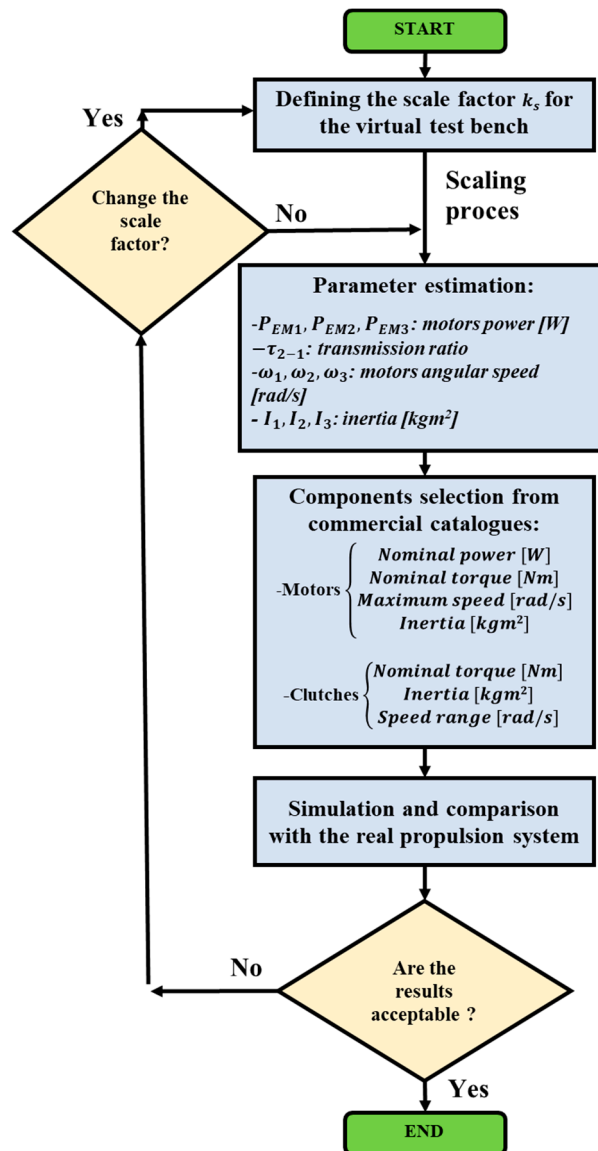


Figure 5. Flow chart of the scaling process.

4. Virtual Test Bench Development

The scaling process for the physical test bench can be directly applied to the virtual test bench as well. The virtual test bench is a high-fidelity mathematical representation of the real test bench built in the simulation environment provided by Matlab/Simulink. The block diagram of the simulation environment is presented in Figure 6, where the mathematical models of the three servomotors EM1, EM2 and EM3 are highlighted. The two electric motors used to simulate the electric drive (EM1) and the ICE (EM2) are considered to be controlled in torque, with their set values defined as a function of the flight segment. The electric motor simulating the propeller behavior EM3 is controlled in speed and its speed set ω_3^{SET} by scaling the angular speed ω_P of the propeller through the gain ω_3/ω_P ; where the angular speed of the propeller is calculated is obtained through a high-fidelity model of the system considering its rotational dynamic equilibrium, the real propeller target speed ω_{TARGET} , aircraft altitude, velocity and the absorbed torque T_P .

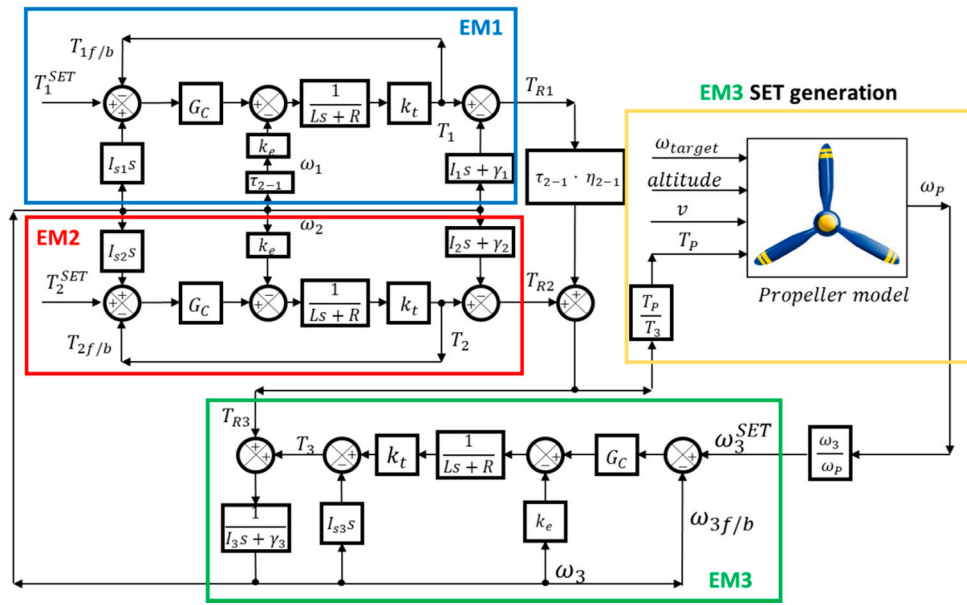


Figure 6. Block diagram of the virtual test bench during the take-off phase.

4.1. Electric Motors

As shown in Figure 6, the three brushless servomotors are modelled as equivalent, monophasic brushless DC-motors through according to the classical equation system reported in [17]:

$$\begin{cases} V = Ri + L \frac{di}{dt} + k_e \omega \\ T = k_t i \\ T - T_R = I_M \frac{d\omega}{dt} + \gamma_M \omega \end{cases} \quad (14)$$

where V is the supply voltage and i is the phase current. The windings resistance R and inductance L as well as the motor speed and torque constants k_e and k_t , are function of the chosen set temperature. I_M is the rotor inertia, γ_M is the viscous damping coefficient, also dependent on temperature, T is the electromechanical torque and T_R is the external torque. A functional model of the electronic power unit interfacing with the battery is added as well, according to the mathematical description provided in [18].

4.2. Propeller

Figure 7 shows the schematics of the propeller model. The model requires in input the propeller pitch, which is function of the difference between the target speed and the current angular speed, the aircraft velocity and the altitude. The propeller model determines thrust force F , the absorbed torque T_P and the efficiency η following the equations described in [19–21] and hereby reported:

$$F = \rho \cdot n_p^2 \cdot c_t \cdot D^4 \quad (15)$$

$$T_P = \rho \cdot n_p^2 \cdot c_p \cdot D^5$$

$$\eta = \frac{F \cdot v}{T_P \cdot 2 \cdot \pi \cdot n_p} = \frac{c_t \cdot v}{n_p \cdot c_p \cdot D \cdot 2 \cdot \pi} \quad (17)$$

where ρ is the air density, c_p is the torque coefficient, c_t is the thrust coefficient, D is the propeller diameter and n_p is the propeller angular speed.

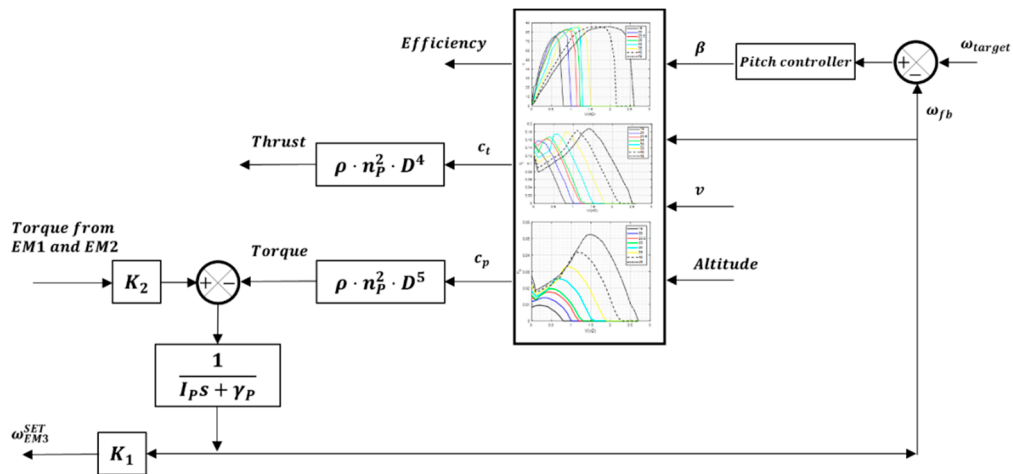


Figure 7. Schematics of the propeller model.

The torque exerted by servomotors EM1 and EM2 is multiplied by the K_2 gain in order to supply the propeller model with the torque in real flight conditions. Similarly, the same process is applied for speed by the K_1 gain, defined as:

$$K_2 = \frac{T_P}{T_3} \quad (18)$$

$$K_1 = \frac{\omega_3}{\omega_p} \quad (19)$$

The model of the pitch controller, depicted in Figure 8, makes use of a purely proportional law with gain k_p to regulate the pitch angle of the propeller around the offset value β_{rif} as a function of the required speed.

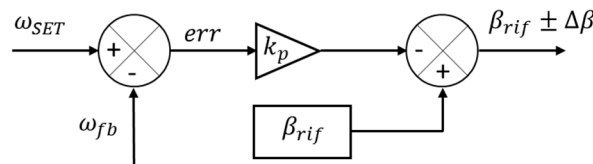


Figure 8. Pitch controller.

4.3. Battery Model

A battery model is included within the environment to simulate the power required by the electric motor-generator installed on the real propulsion system. The model receives the current coming from EM1 motor drive and determines the charge or discharge percentage via the state of charge (SOC) equations. During the charge phase, its percentage value can be computed:

$$SOC [\%] = SOC_{t0} + \frac{100}{C_b} \int_{t0}^{t1} I_{batt} dt \quad (20)$$

While during the discharge phase it is evaluated as:

$$SOC [\%] = SOC_{t0} - \frac{100}{C_b} \int_{t0}^{t1} I_{batt} dt \quad (21)$$

where C_b is the battery capacity and SOC_{t0} is the initial state of charge. The absorbed current I_a can be computed as a function of the supply voltage V_a , the battery efficiency η_b and is the battery tension V_{batt} :

$$I_{batt} = \frac{V_a \cdot I_a}{\eta_b V_{batt}} \quad (22)$$

The implementation of this model, reported in Figure 9, highlights the possibility to introduce the experimentally obtained characteristics of the battery.

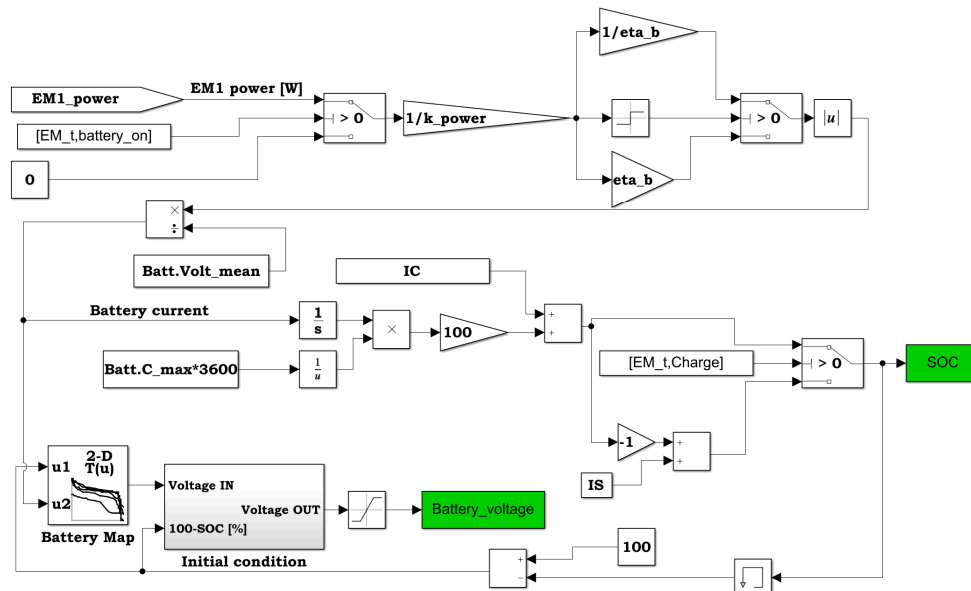


Figure 9. The battery model.

4.4. Simulation of the ICE

The ICE is represented on the test bench by the electric motor EM2. To better mimic the ICE behavior it is possible to add the simulation of the torque ripple typical of ICEs as a function of the angular speed. Referring to Figure 10, the ripple profile is determined by a look up table defined for an 8-cylinder Diesel engine with a displacement of 4089 cm³. The obtained profile is then over imposed on the torque set of the EM2 motor. It is clear that the real-test bench capability to successfully replicate the ripple will be dependent on the dynamic performances of the motor.

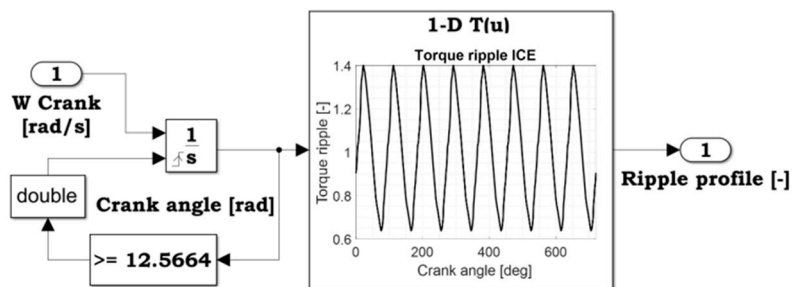


Figure 10. Torque ripple simulation.

5. Application of the Virtual Test Bench

The simulation environment, depicted in Figure 11, is applied to a real propulsion system which requirements, dependent on the flight segment, are reported in Table 2. Six flight phases representative of the UAV application under analysis are considered: green taxi, take-off, climb, ICE heating, cruise and descent. The most demanding condition is the take-off, for which both the electric motor and the

ICE operate at nominal power. The ICE is instead excluded during taxi and descent, while it drags the electric drive during climb and cruise segments allowing for battery recharge. The duration of the ICE heating has been shortened with respect to the real case scenario by generating high torque values to reduce the simulations length. At first, these requirements must be converted into the scaled-down values used in the real (and hence the virtual) test bench, applying the methodology reported in Section 3 for $k_s = 0.0102$. Results are reported in Table 3.

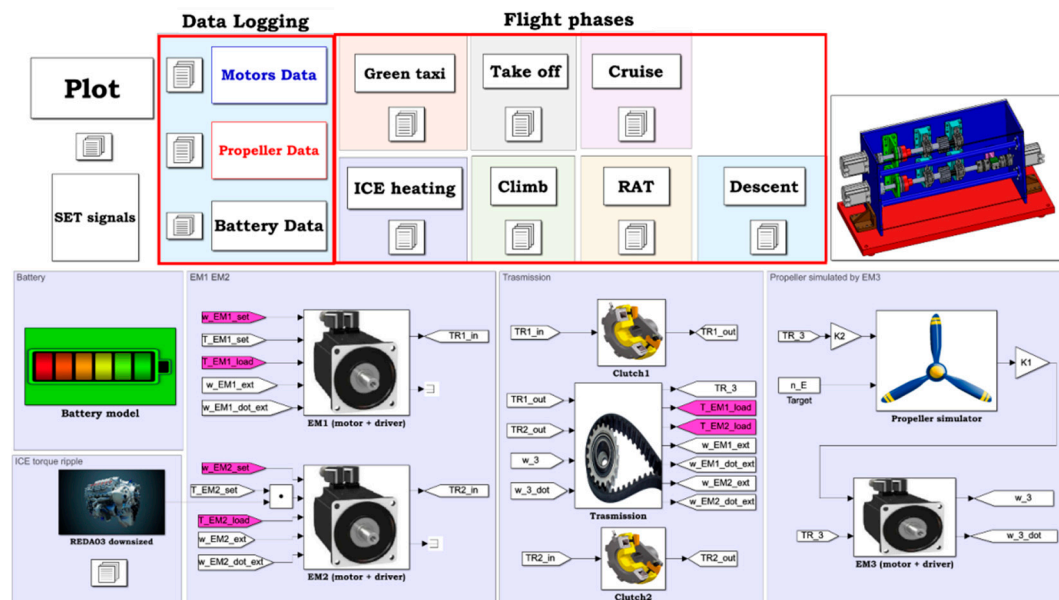


Figure 11. The virtual test bench.

Table 2. Requirements for the real hybrid propulsion system.

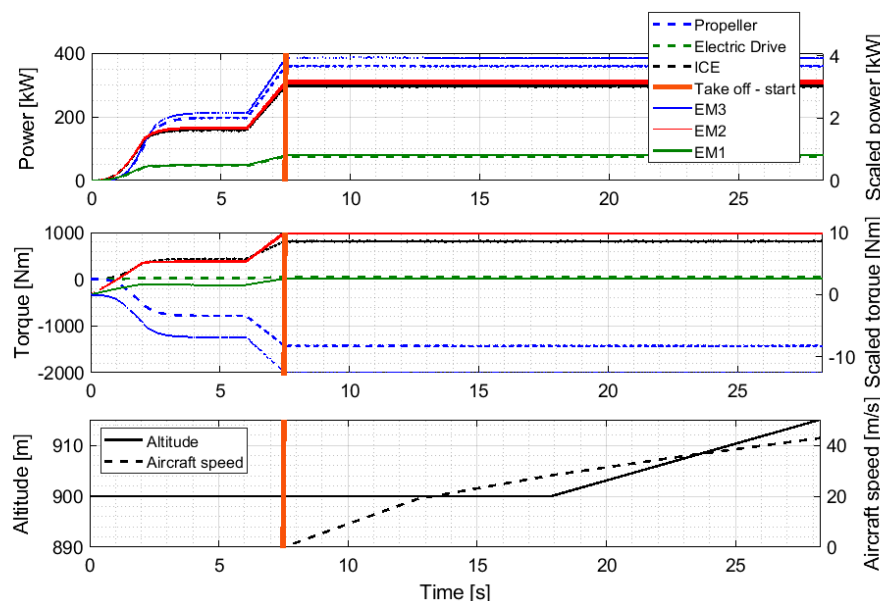
Component/Requirements			Taxi	Take-Off	Climb	ICE Heating	Cruise	Descent
ICE	Target speed	[rpm]	0	3500	3500	3500	3500	0
	Propulsion power	[kW]	0	298	263	159	143	0
	Power to drag EM	[kW]	0	0	11.4	15.9	15.9	0
	Total power	[kW]	0	298	274.42	215.9	158.9	0
	Torque	[Nm]	0	813.47	749.09	589.35	433.76	0
EM	Target speed	[rpm]	6044.4	16,100	16,100	16,100	16,100	16,100
	Mechanical power	[kW]	23.6	76.1	0	0	0	76.1
	Secondary power	[kW]	0	0	10	14	14	0
	Torque	[Nm]	37.3	45,16	5.93	8.31	8.31	45.16
Propeller	Target speed	[rpm]	900	2400	2400	2400	2400	2400
	Power	[kW]	20.7	358.76	258.53	196.60	140.57	65.8
	Torque	[Nm]	220	1428.19	1029.18	781	557.77	262

Table 3. Requirements for the real and the virtual test bench.

Component/Requirements			Taxi	Take-Off	Climb	ICE Heating	Cruise	Descent
ICE	Target speed	[rpm]	0	3000	3000	3000	3000	0
	Propulsion power	[kW]	0	3.04	2.77	2.11	1.507	0
	Power to drag EM	[kW]	0	0	0.12	0.168	0.168	0
	Total power	[kW]	0	3.04	2.89	2.276	1.675	0
	Torque	[Nm]	0	10	9.2	7.23	5.33	0
EM	Target speed	[rpm]	1000	3000	3000	3000	3000	3000
	Mechanical power	[kW]	0.248	0.802	0	0	0	0.80
	Secondary power	[kW]	0	0	0.105	0.147	0.147	0
	Torque	[Nm]	2.37	2.55	0.334	0.468	0.468	2.54
Propeller	Target speed	[rpm]	1000	3000	3000	3000	3000	3000
	Power	[kW]	0.243	3.93	2.77	2.12	1.52	0.783
	Torque	[Nm]	2.32	12.503	8.83	6.74	4.83	2.49

To evaluate the proposed design methodology we compared the expected behavior of a high-fidelity dynamic model of the hybrid propulsion system with the results of the simulated scaled test bench, taking the take-off scenario as the reference case. Both the electric motor and the ICE are active during this phase, hence providing the most amount of information on the virtual test bench behavior.

During the first stages of the simulation, as shown in Figure 12, the propeller is rotated to the target angular speed of 2400 rpm by the combined effort of the ICE and the electric motor. Hence, around the 6 s mark, both the electric motor and the ICE are brought to maximum exerted power conditions and the take-off maneuver is started.

**Figure 12.** Comparison between simulated behavior of the real propulsion system and the scaled virtual test bench.

Eventually the variation of some parameters at aircraft level, i.e., the airplane altitude and speed, is generated. It is worth noting that the speed profile and altitude are external inputs, as an aircraft mathematical model is not implemented within the virtual test bench.

The signals associated with the three electric motor simulated on the scaled-down virtual test bench closely follow the behavior of the real components of the propulsion system; where present, small variations are caused by the difference between the efficiency of the component employed in the real propulsion system and those defined for the test bench. The scaling process is quite successful for the electric motors used to simulate the electric drive and the ICE, while small deviations can be observed

for the propeller. These deviations are mostly due to the control system and the differences between the mechanical characteristics of the propeller and of the electric motor. Although the test-bench makes use of a model of the propeller to define the speed command imposed on EM3, the torque effectively exerted by the electric motor is not directly controlled and hence depends only on the physical properties of the device. This behavior is expected and does not represent an issue for the test-bench, which purpose is to test the propulsion system and the feasibility of its architecture, not the propeller aerodynamics. On the subject of the propulsion system, the scaling process is able to successfully reproduce both the static and the dynamic behavior of the electrical drive and of the ICE; the capability to recreate the dynamic behavior of the real components after the scale-down is of particular interest, since it allows to use the test-bench to study the coupling between the electric drive and the ICE, providing additional information useful for the definition of the mechanical transmission. Figure 13 depicts the behavior of other simulated components, such as the battery (Figure 13a) and the propeller (Figure 13b,c) which output is used to control the EM3.

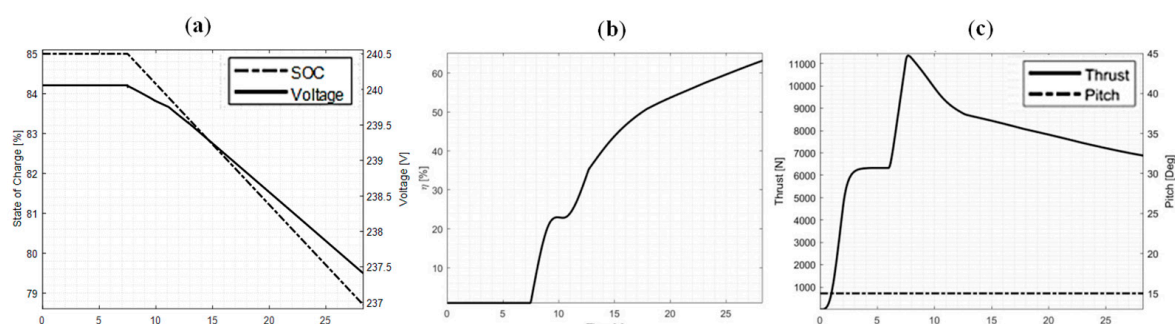


Figure 13. Behavior of significant simulated signals: (a) Battery SOC and Voltage (b) Propeller efficiency (c) Propeller thrust and pitch.

6. Conclusions

This paper proposes a new methodology for the architectural definition and the design of a virtual test bench for an aeronautical hybrid propulsion system, with the aim of supporting the test bench design and, when validated, generate additional synthetic data. The results of the scaling procedure have been compared with those coming from a high-fidelity simulation of the propulsion system under development. Results shows that the scaling of the inertial parameters of the different moving parts allows one to successfully replicate not only scaled-down steady state conditions, but also to closely mirror the expected dynamic behavior of the propulsion system.

The parametrization of the scale factor allows to easily prototype virtual test benches and test their behavior depending on the contextual need of the facility in which the real test bench is going to be installed (i.e., available electrical power, supply voltage...) hence providing a flexible tool for the preliminary design of the real test bench and the choice of its components. Further activities directed at the automatization of the scaling process and the optimization of the scale factor are underway.

Author Contributions: Each author contributed equally to the study object of this paper.

Funding: The research work was performed within the TIVANO project (Innovative Technologies for General Aviation Aircraft of New Generation) lead by Leonardo Aircraft Division (formerly Alenia Aermacchi) funded by Italian Ministry of Education and Research MIUR, call National Aerospace Technology Cluster CTNA, 2014–2017.

Acknowledgments: Authors would like to thank Leonardo Aircraft Division for their support during the development of the research programme.

Conflicts of Interest: The authors declare no conflict of interest.

References

1. Hannan, M.A.; Azidin, F.A.; Mohamed, A. Hybrid electric vehicles and their challenges: A review. *Renew. Sustain. Energy Rev.* **2014**, *29*, 135–150. [[CrossRef](#)]

2. Pornet, C.; Isikveren, A.T. Conceptual design of hybrid-electric transport aircraft. *Prog. Aerosp. Sci.* **2015**, *79*, 114–135. [[CrossRef](#)]
3. Isikveren, A.T.; Kaiser, S.; Pornet, C.; Vratny, P.C. Pre-design strategies and sizing techniques for dual-energy aircraft. *Aircr. Eng. Aerosp. Technol.* **2014**, *86*, 525–542. [[CrossRef](#)]
4. Bagassi, S.; Bertini, G.; Francia, D.; Persiani, F. Design Analysis for Hybrid Propulsion. In Proceedings of the 28th International Congress of the Aeronautical Sciences, Brisbane, Australia, 23–28 September 2012.
5. Hung, J.Y.; Gonzalez, L.F. On parallel hybrid-electric propulsion system for unmanned aerial vehicles. *Prog. Aerosp. Sci.* **2012**, *51*, 1–17. [[CrossRef](#)]
6. Boggero, L.; Fioriti, M.; Ragusa, C.S.; Corpino, S. Trade off studies of hybrid-electric aircraft by Fuzzy Logic methodology. *Int. J. Appl. Electromagn. Mech.* **2018**, *56*, 143–152. [[CrossRef](#)]
7. Boggero, L.; Fioriti, M.; Corpino, S. Development of a new conceptual design methodology for parallel hybrid aircraft. *Proc. Inst. Mech. Eng. Part G J. Aerosp. Eng.* **2019**, *233*, 1047–1058. [[CrossRef](#)]
8. Glasscock, R.; Hung, J.Y.; Gonzalez, L.F.; Walker, R.A. Design, modelling and measurement of a hybrid powerplant for unmanned aerial systems. *Proc. Aust. J. Mech. Eng.* **2008**, *6*, 69–78. [[CrossRef](#)]
9. Lieh, J.; Spahr, E.; Behbahani, A.; Hoying, J. Design of Hybrid Propulsion Systems for Unmanned Aerial Vehicles. In Proceedings of the 47th AIAA/ASME/SAE/ASEE Joint Propulsion Conference & Exhibit, San Diego, CA, USA, 31 July–3 August 2011.
10. *Viable Innovation—Hybrid Drive Propels Light Aircraft, Project Status AERO*; Flight Design gmbH: Hørselberg-Hainich, Germany, 2010.
11. Friedrich, C.; Robertson, P.A. Hybrid-Electric Propulsion for Aircraft. *J. Aircr.* **2014**, *52*, 176–189. [[CrossRef](#)]
12. Friedrich, C.; Robertson, P.A. Hybrid-electric propulsion for automotive and aviation applications. *CEAS Aeronaut. J.* **2015**, *6*, 279–290. [[CrossRef](#)]
13. Schupbach, R.M.; Balda, J.C. A versatile laboratory test bench for developing powertrains of electric vehicles. In Proceedings of the IEEE 56th Vehicular Technology Conference, Vancouver, BC, Canada, 24–28 September 2003.
14. Hui, Z.; Cheng, L.; Guojian, Z. Design of a versatile test bench for hybrid electric vehicles. In Proceedings of the 2008 IEEE Vehicle Power and Propulsion Conference, Harbin, China, 3–5 September 2008.
15. Jacazio, G.; Balossini, G. A high performance force control system for dynamic loading and fast moving actuators. In *Power Transmission and Motion Control*; Wiley: Hoboken, NJ, USA, 2005.
16. Bertucci, A.; Mornacchi, A.; Jacazio, G.; Sorli, M. A Force Control Test Rig for the Dynamic Characterization of Helicopter Primary Flight Control Systems. *Procedia Eng.* **2015**, *106*, 71–82. [[CrossRef](#)]
17. Jones, B.L. Power Electronics and AC Drives. *Power Eng. J.* **2009**, *1*, 125. [[CrossRef](#)]
18. Mohan, N. *Power Electronics—A first Course*; Wiley: Hoboken, NJ, USA, 2013; ISBN 97811180748000.
19. Wald, Q.R. The aerodynamics of propellers. *Prog. Aerosp. Sci.* **2006**, *42*, 85–128. [[CrossRef](#)]
20. Hoelzen, J.; Liu, Y.; Bensmann, B.; Winnefeld, C.; Elham, A.; Friedrichs, J.; Hanke-Rauschenbach, R. Conceptual design of operation strategies for hybrid electric aircraft. *Energies* **2018**, *11*, 217. [[CrossRef](#)]
21. Selig, M. Modeling Propeller Aerodynamics and Slipstream Effects on Small UAVs in Realtime. In Proceedings of the AIAA Atmospheric Flight Mechanics Conference, Minneapolis, MN, USA, 13–16 August 2012.



© 2019 by the authors. Licensee MDPI, Basel, Switzerland. This article is an open access article distributed under the terms and conditions of the Creative Commons Attribution (CC BY) license (<http://creativecommons.org/licenses/by/4.0/>).